

The Cost of Cortical Computation

Peter Lennie*

Center for Neural Science
New York University
4 Washington Place
New York, New York 10003

Summary

Electrophysiological recordings show that individual neurons in cortex are strongly activated when engaged in appropriate tasks, but they tell us little about how many neurons might be engaged by a task, which is important to know if we are to understand how cortex encodes information. For human cortex, I estimate the cost of individual spikes, then, from the known energy consumption of cortex, I establish how many neurons can be active concurrently. The cost of a single spike is high, and this severely limits, possibly to fewer than 1%, the number of neurons that can be substantially active concurrently. The high cost of spikes requires the brain not only to use representational codes that rely on very few active neurons, but also to allocate its energy resources flexibly among cortical regions according to task demand. The latter constraint explains the investment in local control of hemodynamics, exploited by functional magnetic resonance imaging, and the need for mechanisms of selective attention.

Introduction

The coding principles used to represent sensory information in the cortex are not well understood. Although it is widely agreed that the analysis is organized in distinct modules, within a system that is both parallel and hierarchical [1], we know relatively little about the roles of individual neurons. In particular, we do not know whether a representation involves activity in many or few neurons. Barlow [2, 3] argued that very few active neurons were used, but this proposition has never been systematically evaluated. It has now become tractable. In what follows, I use recent analyses of energy consumption to estimate the normally sustainable spiking activity in neurons of human neocortex. I show that neural activity is very costly, and that a little of it has to go a long way.

Results and Discussion

The Cost of a Spike

The cost of a spike arises in restoring ionic balances perturbed by synaptic potentials and the action potential and in the release and reuptake of neurotransmitter at synapses. Attwell and Laughlin [4] made a detailed biophysical analysis of these costs for a single neuron in

rat neocortex. Neurons in human neocortex are larger than those in rat and receive and make more synapses, but they are not otherwise known to differ in their basic structure or organization [5]. Thus, with appropriate scaling of parameters for the larger neurons, Attwell and Laughlin's analysis can be used to estimate the energy consumed by a pyramidal neuron in human neocortex.

In different mammals, the number of neurons under a unit area of cortical surface is relatively constant ($\sim 100,000/\text{mm}^2$), except in primate striate cortex, where it may be twice as high [6]. Increasing brain size brings an increase in cortical thickness and a proportionately lower density of neurons [5, 6] without an increase in cell body size, which remains approximately constant at $15\ \mu\text{m}$ diameter [7]. The volume of axons and dendrites increases with cortical thickness. This reflects an increase in the lengths of dendrites and axons without an increase in diameter [5]. Table 1 summarizes relevant statistics for human cortex.

Postsynaptic Potentials

Individual synapses are assumed to be the same in rat and human neurons, so the energy costs associated with transmitter uptake and release will be the same, as will the current flow through receptor channels. Given (from Table 1) 7×10^8 synapses per mm^3 of cortex, and $40,000$ neurons/ mm^3 , the average neuron will make $17,500$ synaptic contacts. If we use this number, and assume a 50% failure rate [8, 9], the cost of EPSPs arising from a single spike will be 1.2×10^9 ATP molecules [4].

Spike Propagation

The cost of propagating an action potential in an unmyelinated axon is proportional to its surface area. The same principle holds for action potential invasion of the soma and dendrites. From Table 1, the average cell has $100\ \text{mm}$ of intracortical axon (axon collaterals confined to gray matter; the analysis ignores myelinated segments of axon that leave cortex and reenter it) and $10\ \text{mm}$ of dendrites. These lengths are 2.5 times greater than in rodent [5], and the spike propagation cost (9.2×10^8 ATP molecules per spike [4]) is correspondingly greater.

Neurotransmitter Release and Recycling

Calcium influx associated with release of a vesicle, exocytosis and endocytosis, and the uptake conversion and recycling of a glutamate molecule by an astrocyte altogether consume 2.3×10^4 ATP per vesicle released [4]. With a 50% failure rate at $17,500$ synapses, the overall cost of recycling glutamate released by a spike will be 2.1×10^9 ATP.

The aggregate cost of a spike is 2.4×10^9 ATP molecules. Figure 1A shows the breakdown of component costs. For the average pyramidal cell, the largest cost is EPSPs, followed by the cost of transmission along the axon. Transmitter release and recycling each ac-

*Correspondence: pl@cns.nyu.edu

Table 1. Basic Statistics of Human Neocortex

Property	Value	Source
Surface area (mm ²)	190,000	[7, 24]
Thickness (mm)	2.5	[6, 25]
Glucose Consumption (μmol/g/min)	0.40	[10–12]
Glia/mm ³	38,000	[7]
Neurons/mm ³	40,000	[6, 26]
Synapses/mm ³	7×10^8	[5, 27, 28]
Axon Length m/mm ³	4,000	[5]
Average Axon Diameter (μm)	0.3	[5]
Dendrite Length m/mm ³	400	[5]
Average Dendrite Diameter (μm)	0.9	[5]

count for about 4% of the total cost. The overall cost in a human cell is 3.3 times that in rat [4]; the human neuron has more synapses that are assumed to be more reliable and has longer dendrites and axon collaterals.

Sustainable Spike Rate

Positron emission tomography (PET) and Magnetic Resonance Spectroscopy (MRS) measurements of glucose metabolism in human cortex show overall resting consumption of about 0.40 μmol/g/min [10–12]. Assuming a yield of 30 ATP per molecule of glucose [13], this would give rise to 12 μmol ATP/g/min. With 1 cm³ of cortex weighing 1 g [14], from Table 1, the cortical mass is 475 g, resulting in a gross consumption of 3.4×10^{21} molecules of ATP per minute.

We want to identify the energy expenditures related to neural signaling. The principal cost of restoring and maintaining ionic balances can be estimated from the decrease in energy consumption brought about by inactivating the Na/K pump with ouabain or an equivalent agent. Doing this reduces overall energy consumption

by about 50% [15]. Ion pumping therefore consumes 1.7×10^{21} ATP molecules/min. Expenditures that are unrelated to signaling arise principally in axonal and dendritic transport, intracellular signaling, and vegetative metabolism [15].

The Na/K pump supports not only spikes, but also the resting potentials in neurons and glia. The cost of maintaining the resting potential depends on membrane input resistance, which will vary inversely with membrane surface area; thus, for a human neuron, this cost is estimated by multiplying the cost in rat by the ratio of surface areas. For a human neuron, this is 8.6×10^8 ATP/s, and for an astrocyte, it is about 3.1×10^8 ATP/s. Given these expenditures, and the numbers of neurons and glia from Table 1, the cost of maintaining resting potentials in all neurons and glia is 1.3×10^{21} ATP molecules per minute, leaving 3.9×10^{20} per minute to support ionic movements associated with spikes. Figure 1B shows the overall allocation of energy among different functions. Expenditures associated with spiking are identified by segments pulled out from the chart: they account for 13% of the total.

From the previous section, reversing the Na⁺ and K⁺ fluxes moved by a single spike consumes 2.2×10^9 ATP molecules. Given this, and 1.9×10^{10} cortical neurons, the ATP available for the Na/K pump would support an average discharge rate of 0.16 spikes/s/neuron. This is a remarkably small number, with important implications for neural coding. It is therefore important to understand its reliability. A detailed analysis of potential errors provided in the Supplemental Data available with this article online shows that no individual source of uncertainty will have a large effect on the sustainable spike rate. Nevertheless, it is useful to know what sustainable spike rate would result from relatively extreme parameter val-

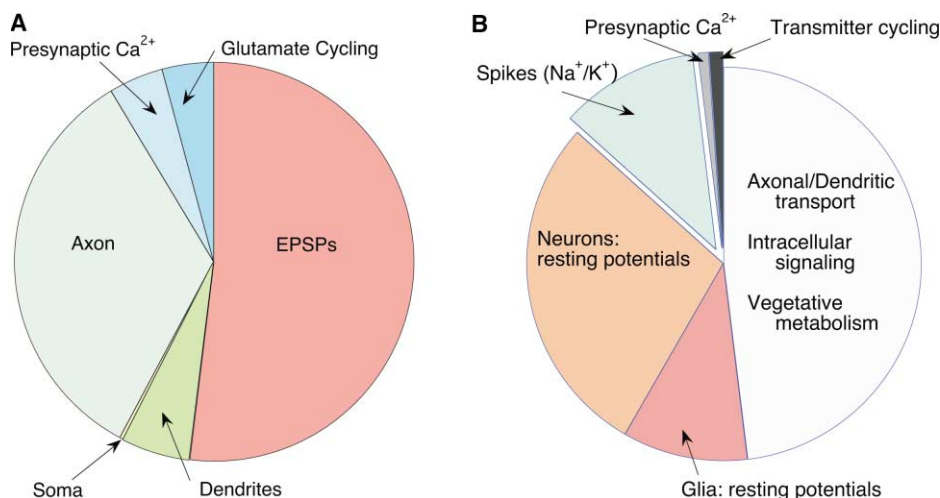


Figure 1. Energy Cost of Neural Activity in Human Cortex

(A) How the cost of a single spike in a human pyramidal cell arises in different processes. A spike consumes 2.4×10^9 molecules of ATP. The principal cost (52%) is EPSPs evoked at postsynaptic sites. Propagation in dendrites and soma account for 6% and 0.25%, respectively. Propagation along the axon accounts for 33%. Mechanisms of transmitter release and recycling consume 5% and 4%, respectively.

(B) Fractions of total energy expenditure in neocortex that are attributable to different functions. Maintaining resting potentials in neurons and glia accounts for 28% and 10%, respectively. Reversing Na⁺ and K⁺ fluxes from spikes accounts for an additional 13%. Calcium movements associated with transmitter release and transmitter recycling each account for less than 1%. Functions unrelated to neural signaling account for the remainder. Segments that represent costs associated with spiking are pulled out from the chart.

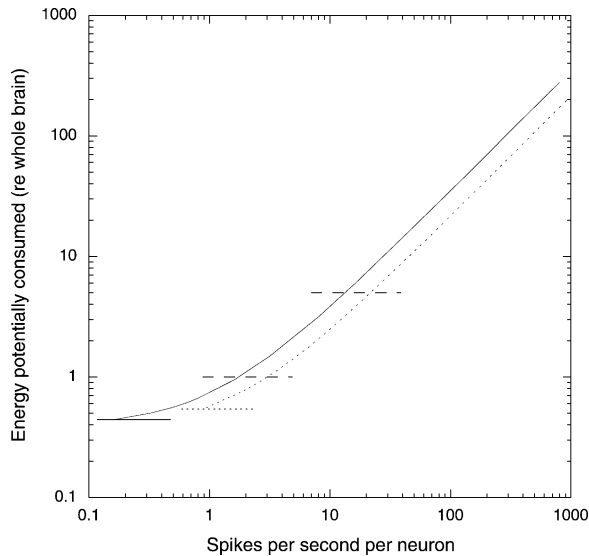


Figure 2. Energy Potentially Consumed by Cortex as a Function of the Average Sustained Level of Activity in All Neurons

Energy consumption, expressed as a fraction of whole brain consumption, is calculated in two ways: the first (solid curve) is based on best estimates of energy availability and costs, and the second (dotted curve) is based on estimates that tend to minimize energy consumption (see text). Using the best estimate, in the normal awake state, cortex accounts for 44% of whole brain energy consumption (solid horizontal line, intercept on ordinate). This supports an average of 0.16 spikes/s/neuron. The total energy consumed would initially grow increasingly rapidly with increasing spike rate, until the spike-dependent costs exceed the fixed costs. To sustain an average rate of 1.8 spikes/s/neuron would use more energy than is normally consumed by the whole brain (solid curve crosses lower dashed line); to sustain an average rate of 13 spikes/s/neuron would use more energy than is normally consumed by the whole body (solid curve crosses upper dashed line). Even with the conservative estimate of energy consumption (dotted curve), sustaining an average rate of 3.1 spikes/s/neuron would use more energy than is normally consumed by the whole brain.

ues that all tend to underestimate the cost of spikes. If synaptic reliability were 0.25, the fraction of axons myelinated 0.25, the average diameter of axons and dendrites 25% greater than in rodent, overall glucose consumption 0.50 $\mu\text{mol/g/min}$, and the fraction of that consumed by the Na/K pump 0.6, then the average sustainable spike rate would rise to 0.94 spikes/s/neuron, which is still a very small number.

Number and Distribution of Active Neurons

Given the volume of human neocortex (Table 1), glucose consumption of 0.40 $\mu\text{mol/g/min}$ will yield a gross consumption of 190 $\mu\text{mol/min}$, or 34 mg/min. From the literature, Clarke and Sokoloff [16] estimate median whole-brain glucose consumption in young adults to be 77 mg/min. Thus, neocortex accounts for 44% of the brain's overall consumption. Knowing this allows us to project how the brain's energy consumption would grow with the number of spikes discharged per second per neuron (Figure 2, solid curve). A 10-fold increase in the average spike rate (to 1.6 spikes/s/neuron) would require more than a 2-fold increase in energy consumed by cortex. Were the average rate 100 spikes/s, energy consump-

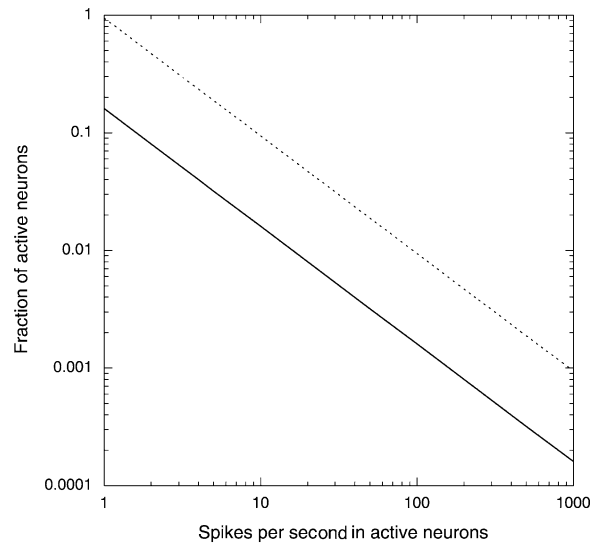


Figure 3. Fraction of Cortical Neurons that Can Be Active, as a Function of the Average Spike Rate in Those Neurons that Are Active
The fraction of active neurons is calculated in two ways: the first (solid line) is based on best estimates of energy availability and costs, and the second (dotted line) is based on estimates that tend to minimize energy consumption (see text). The overall energy consumption of the awake brain is assumed to be fixed and invariant with mental activity. If a strong neural signal is taken to be 10 spikes in 200 ms, the brain's normal energy consumption supports a strong signal in 1 in 312 cortical neurons.

tion would be 79 times higher than normal. These numbers have to be understood in the context of the body's overall energy consumption. In the young human adult, the brain accounts for 20% of the total; in children, the fraction is nearer 50% [16].

The brain's energy consumption does not change with normal variations in mental activity, though it is reduced by sleep and various pathological states [16]. Hence, it seems that in normal operation a limited energy resource must be allocated flexibly among all neurons. Given a fixed supply of energy, the number of neurons that can be active will vary with the average discharge rate in the active ones. Figure 3 shows this relationship. For purposes of illustration, all neurons that are active are assumed to be discharging spikes at the same rate.

In behaving monkeys, neurons engaged in cognitive or sensory-motor tasks can discharge action potentials at rates of up to 100/s, at least for a short time [17–19]. If we take 10 spikes in 200 ms to be a strong signal, then from Figure 3 we see that the available energy supports concurrent signaling in 1 in 312 neurons. This ratio assumes that all but the "working" neurons are completely silent. In sensory cortex, if not elsewhere, neurons are often slightly active even when apparently not engaged in a task, and this will reduce the sustainable number of working neurons.

The very large increase in metabolic demand caused by substantial neural activity and the fact that overall energy consumption is essentially constant necessitate machinery for allocating energy flexibly. The local changes in cerebral hemodynamics associated with neural activity, and exploited in functional magnetic res-

onance imaging (fMRI) [20], are an obvious sign of this. The hemodynamic change is accompanied by a change in glucose consumption, but not on a scale commensurate with a substantial change in the activity of all neurons. This has been studied most thoroughly in visual cortex, where glucose consumption measured by PET and MRS increases by about 50% as visual input changes from impoverished (eyes closed or darkness) to rich (spatiotemporal flicker) [10, 12]. If neurons had no resting discharge, this increase would support an average spike rate of 0.80 spikes/s/neuron (Figure 2) or, put differently, 1 neuron in 63 could be active at 50 spikes/s. Some visual cortical neurons in monkey are spontaneously active, but because these are easily found with single-unit recordings, they are likely to be substantially overrepresented in most studies. Were the average resting rate in the population as high as 3 spikes/s/neuron (the mean discharge rate to uniform illumination in 230 V1 and V2 neurons in lightly anesthetized macaque studied by J. Kraft, J. Peirce, J. Forte, J. Krauskopf, and P.L., unpublished data), a 50% increase in energy consumption would support an average increase in rate of 2 spikes/s/neuron, for a discharge rate of 5 spikes/s/neuron (or 1 neuron in 25 discharging at 50 spikes/s). It therefore seems likely that, even in strongly driven visual cortex, only a small fraction of neurons is working at any one time—between 1 in 25 and 1 in 63, with the latter the more probable value. Heeger et al. [21] reached the same conclusion on quite different grounds. All indications are that sensory cortex is among the most active metabolically, so it is unlikely that there is ever a larger fraction of neurons working concurrently in any other part of the cortex.

An individual spike in human cortex costs 3.3 times more than in rat, and maintaining resting potentials costs 2.6 times as much. Despite this, the rate of glucose metabolism in human cortex [10–12] is three times lower than in rat [16], and about 1.5 times lower than in monkey [16]. The implication is that many fewer neurons are active in human cortex.

Consequences of Expensive Spikes

Levy and Baxter [22] noted that the relative cost of spikes (versus silence) will determine how many concurrently active neurons provide the energetically optimal encoding of a stimulus. Their analysis shows generally that the more expensive spikes are, the smaller the optimal fraction of active neurons. From the analysis offered here, the cost of 10 spikes in 200 ms is more than 100 times that of maintaining the resting potential, and the optimal fraction of active neurons is about 3% [22]. A similar model for assessing the energetically optimal sparseness of representation [4] would put the optimal fraction of active neurons at between 1% and 4%, for a group of neurons that can represent between 100 and 1000 distinct entities. These results endorse the representational scheme first proposed by Barlow [2, 3] on quite different grounds.

Even with only a few percent of neurons concurrently active in any local region, the metabolic burden would be unsustainable over all of cortex. If the cost estimate offered here is broadly correct, and if just 3% of neurons

were concurrently firing (at 10 spikes in 200 ms) in “active” cortex, less than 10% of cortex could be active at all. This must limit the range of tasks that can be undertaken concurrently, and it necessitates machinery for allocating energy according to task demand. The need for energy management provides an interesting physiological perspective on a traditional view of attention as an adaptation to the brain’s limited capacity to process information [23]: energy limitations require that only a small fraction of the machinery can ever be engaged concurrently. The scarcity of spikes does not imply that only one or a few tasks can be undertaken concurrently, but it does imply a cap on the aggregate neural activity and provides a natural metric for characterizing aggregate task difficulty: how much cortex is active.

Supplemental Data

Supplemental Data provides an analysis of potential errors in the estimate of sustainable spike rates and is available at <http://images.cellpress.com/supmat/supmatin.htm>.

Acknowledgments

This work was supported by National Institutes of Health grants EY04440 and EY13079. I am grateful to D. Attwell, M. Carrasco, G. Elston, N. Graham, D. Heeger, J. Krauskopf, S. Laughlin, N. Logothetis, J. Maunsell, J. Movshon, J. Müller, and J. Rinzal for discussion and comment and to M. Häusser and A. Roth for help in estimating the cost of spike propagation in myelinated axons.

Received: September 13, 2002

Revised: January 15, 2003

Accepted: January 15, 2003

Published: March 18, 2003

References

1. Lennie, P. (1998). Single units and visual cortical organization. *Perception* 27, 889–935.
2. Barlow, H.B. (1961). The coding of sensory messages. In *Current Problems in Animal Behaviour*, W.H. Thorpe and O.L. Zangwill, eds. (Cambridge: Cambridge University Press), pp. 331–360.
3. Barlow, H.B. (1972). Single units and sensation: a neuron doctrine for perceptual psychology? *Perception* 1, 371–394.
4. Attwell, D., and Laughlin, S.B. (2001). An energy budget for signaling in the grey matter of the brain. *J. Cereb. Blood Flow Metab.* 21, 1133–1145.
5. Braitenberg, V., and Schütz, A. (1998). *Cortex: Statistics and Geometry of Neuronal Connectivity*, Second Edition (Berlin: Springer).
6. Rockel, A.J., Hiorns, R.W., and Powell, T.P.S. (1980). The basic uniformity in structure of the neocortex. *Brain* 103, 221–244.
7. Haug, H. (1987). Brain sizes, surfaces, and neuronal sizes of the cortex cerebri: a stereological investigation of man and his variability and a comparison with some mammals (primates, whales, marsupials, insectivores, and one elephant). *Am. J. Anat.* 180, 126–142.
8. Markram, H., Lübke, J., Frotscher, M., Roth, A., and Sakmann, B. (1997). Physiology and anatomy of synaptic connections between thick tufted pyramidal neurones in the developing rat neocortex. *J. Physiol.* 500, 409–440.
9. Hardingham, N.R., and Larkman, A.U. (1998). The reliability of excitatory synaptic transmission in slices of rat visual cortex *in vitro* is temperature dependent. *J. Physiol.* 507, 249–256.
10. Fox, P.T., Raichle, M.E., Mintun, M.A., and Dence, C. (1988). Nonoxidative glucose consumption during focal physiologic neural activity. *Science* 241, 462–464.
11. Shen, J., Petersen, K.F., Behar, K.L., Brown, P., Nixon, T.W., Mason, G.F., Petroff, O.A., Shulman, G.I., Shulman, R.G., and

- Rothman, D.L. (1999). Determination of the rate of the glutamate/glutamine cycle in the human brain by *in vivo* ^{13}C NMR. *Proc. Natl. Acad. Sci. USA* 96, 8235–8240.
12. Chhina, N., Kuestermann, E., Halliday, J., Simpson, L.J., Macdonald, I.A., Bachelard, H.S., and Morris, P.G. (2001). Measurement of human tricarboxylic acid cycle rates during visual activation by ^{13}C magnetic resonance spectroscopy. *J. Neurosci. Res.* 66, 737–746.
 13. Stryer, L. (1995). *Biochemistry*, Fourth Edition (New York: Freeman).
 14. Stephan, H., Frahm, H., and Baron, G. (1981). New and revised data on volumes of brain structures in insectivores and primates. *Folia Primatol.* 35, 1–29.
 15. Ames, A., III. (2000). CNS energy metabolism as related to function. *Brain Res. Rev.* 34, 42–68.
 16. Clarke, D.D., and Sokoloff, L. (1994). Circulation and energy metabolism of the brain. In *Basic Neurochemistry*, G.J. Siegel, B.W. Agranoff, R.W. Albers, and P.B. Molinoff, eds. (New York: Raven), pp. 645–680.
 17. Miller, E.K., Erickson, C.A., and Desimone, R. (1996). Neural mechanisms of visual working memory in prefrontal cortex of the macaque. *J. Neurosci.* 16, 5154–5167.
 18. DiCarlo, J.J., and Maunsell, J.H. (2000). Form representation in monkey inferotemporal cortex is virtually unaltered by free viewing. *Nat. Neurosci.* 3, 814–821.
 19. Sheinberg, D.L., and Logothetis, N.K. (2001). Noticing familiar objects in real world scenes: the role of temporal cortical neurons in natural vision. *J. Neurosci.* 21, 1340–1350.
 20. Heeger, D.J., and Ress, D. (2002). What does fMRI tell us about neuronal activity? *Nat. Rev. Neurosci.* 3, 142–151.
 21. Heeger, D.J., Huk, A.C., Geisler, W.S., and Albrecht, D.G. (2000). Spikes versus BOLD: what does neuroimaging tell us about neuronal activity? *Nat. Neurosci.* 3, 631–633.
 22. Levy, W., and Baxter, R.A. (1996). Energy-efficient neural codes. *Neural Comput.* 8, 531–543.
 23. Broadbent, D.E. (1971). *Decision and Stress* (London: Academic Press).
 24. Tramo, M.J., Loftus, W.C., Thomas, C.E., Green, R.L., Mott, L.A., and Gazzaniga, M.S. (1995). Surface area of human cerebral cortex and its gross morphological subdivisions: *in vivo* measurements in monozygotic twins suggest differential hemisphere effects of genetic factors. *J. Cogn. Neurosci.* 7, 292–302.
 25. Fischl, B., and Dale, A.M. (2000). Measuring the thickness of the human cerebral cortex from magnetic resonance images. *Proc. Natl. Acad. Sci. USA* 97, 11050–11055.
 26. Braendgaard, H., Evans, S.M., Howard, C.V., and Gundersen, H.J. (1990). The total number of neurons in the human neocortex unbiasedly estimated using optical disectors. *J. Microsc.* 157, 285–304.
 27. Cragg, B.G. (1975). The density of synapses and neurons in normal, mentally defective ageing human brains. *Brain* 98, 81–90.
 28. Abeles, M. (1991). *Corticonics* (Cambridge: Cambridge University Press).

The Cost of Cortical Computation

Peter Lennie

Supplemental Results and Discussion

The measurements and assumptions that drive estimates of the energy consumed by neuronal activity in human cortex are subject to error. The following paragraphs explore some sources of uncertainty and their likely effects on sustainable spike rates.

Area and Thickness of Cortex

Estimates of cortical surface area range from about 160,000 mm² to 250,000 mm² [S1, S2]. The variation among individuals is real: much of this range can be found in a single study of 20 brains [S2]. The value used here (190,000 mm²) is the average. Different measurements of cortical thickness agree well, on an average of 2.5 mm [S3]. The volume of neocortex estimated from average surface area and thickness is 475,000 mm³, about 37% of total brain weight. This is about half the volume found by Stephan [S4] in a single brain by using different methods. To the extent that the volume of cortex is underestimated, the gross metabolic demand will be underestimated. This becomes an issue only if the brain's overall energy consumption is limited.

Densities of Synapses and Neurons

Estimates of synaptic density are quite uniform at $6\text{--}8 \times 10^8/\text{mm}^3$ [S5, S6]. Estimates of neuron density in human cortex (excluding striate cortex) vary from $1.1 \times 10^4/\text{mm}^3$ to $6 \times 10^4/\text{mm}^3$ (values tabulated by Abeles [S5]). The estimate of 4×10^4 used here [S7] is near the middle of the range and is consistent with the value obtained by dividing the overall volume of cortex ($\sim 500,000 \text{ mm}^3$) by the total neuron count ($\sim 2 \times 10^{10}$) estimated by a variety of means [S8, S9]. In any case, the energy cost is quite insensitive to neuron density, because the preponderant costs arise in axons and dendrites, whose total surface area is independent of neuron density, and at synapses, whose number is independent of neuron density. A 2-fold reduction in the density of neurons would increase the sustainable number of spikes to 0.23 spikes/s/neuron.

Types of Neurons and Synapses

Pyramidal cells provide the principal excitatory drive in cortex. Various estimates put their proportion at 85%–90% of cortical neurons [S6, S10, S11], with stellate cells constituting most of the remainder. Stellate cells have 2/3 the dendritic length of pyramidal cells [S6], but this is already factored into the average dendritic length used in estimating spike costs. Stellate cells discharge briefer spikes [S12], so their costs might be a little lower. Some make inhibitory (type II) synapses, and these might have a slightly lower cost than excitatory ones [S13]. Even if the cost of a spike in a stellate cell were as little as half that in a pyramidal cell, the average sustainable spike rate would rise to only 0.17 spikes/s/neuron.

Reliability of Synapses

The reliability of synaptic transmission depends on presynaptic spike rate. When spikes are infrequent, failure rates in neocortex at or near normal body temperature are lower than 20% [S14, S15], so the value used here (50%) is conservative. In any case, the reliability of transmission has relatively little impact on the overall sustainable spike rate: a 20% failure rate puts the sustainable spike rate at 0.12 spikes/s/neuron; a failure rate of 80% puts the sustainable spike rate at 0.24 spikes/s/neuron.

Na⁺ Currents

The estimate of charge moved during an EPSP (6.7×10^{-14} Coulombs) is slightly lower than other estimates [S16, S17]. Given the lower membrane resistance of the human neuron, the resulting EPSP would be smaller than in the rat, and a greater number of active

synapses would be required to trigger a spike. If in fact EPSPs were the same size in rat and human neurons, the scaling principle used here would underestimate their cost. The estimate of charge moved in the axon during spike propagation (3.8×10^{-10} Coulombs) is at the low end of the range typical for unmyelinated fiber of the same area [S18]. The cost of maintaining resting potentials is less firm. The values provided here assume an input resistance higher than has generally been found experimentally [S19]; if input resistance has been overestimated, the cost of the resting potential will have been underestimated and the sustainable spike rate overestimated.

Myelinated Axons

Some unknown number of intracortical axons are myelinated [S20]. Little is known about their biophysical properties, but an implementation by M. Häusser and A. Roth (personal communication) of the model pyramidal cell developed by Mainen et al. [S21], and applied to axons 100 mm long, shows the cost of propagating a spike to be $1.8 \times 10^9 \text{ Na}^+$ (76% of the cost in an unmyelinated fiber). Even if all intracortical axons were myelinated, given the costs noted, the overall sustainable spike rate would rise only to 0.18 spikes/s/neuron.

Dimensions of Axons and Dendrites

The average dimensions of axons and dendrites are important determinants of signaling costs. These are known reliably for rodent [S6], but less so for the thicker human cortex. The key assumption is that the increased thickness of cortex results in proportionately longer, but not thicker, processes. Three kinds of evidence endorse this. First, direct measurements show that (other than in V1) the total length of a pyramidal cell's basal dendrites in human cortex is 5–6 mm [S22]. Basal dendrites account for 55% of the total dendritic length [S23], so the total length is ~ 10 mm, as expected from scaling values from rodent. Second, axon diameter is approximately proportional to cell body size [S24], but cell bodies in human neocortex are no larger than are those in rodents [S1]. Third, the density of spines on dendrites is proportional to dendrite diameter [S25]. The average density of synapses on dendrites is quite constant across species [S26]. In human pyramidal cells, it varies between 1 and $2.5/\mu\text{m}$, depending on cortical region [S22]; the overall value for mouse is $2/\mu\text{m}$ [S6]. When coupled with the observation that the number of synapses per unit volume of cortex is constant across species, the constant density of synapses on dendrites implies that the length of dendrites per unit volume is the same in human and rodent cortex. Nevertheless, if axon collaterals and dendrites in human were as much as 25% thicker than those of rodent, while occupying constant volume, the average sustainable spike rate would rise only to 0.26 spikes/s/neuron.

Available Energy

The energy available to support spiking is found by establishing the overall energy consumption of cortex and by then subtracting identified expenditures unrelated to signaling. Different estimates of cortical glucose consumption agree well, though they tend to emphasize sensory cortex. The value assumed here ($0.40 \mu\text{mol/g/min}$) is mid-range. If consumption were as much as $0.60 \mu\text{mol/g/min}$ (the high value in the literature [S27]), the sustainable average spike rate would be 0.51 spikes/s/neuron. The fraction of ATP consumed by the Na/K pump is less certain. Values in the literature range from 40% to 60%. If the fraction were as low as 40%, the sustainable spike rate (given the estimated cost of resting potentials) would fall to 0.02 spikes/s/neuron; if the value were as high as 60% the average sustainable rate would be 0.30 spikes/s/neuron.

Supplementary References

- S1. Haug, H. (1987). Brain sizes, surfaces, and neuronal sizes of the cortex cerebri: a stereological investigation of man and his

- variability and a comparison with some mammals (primates, whales, marsupials, insectivores, and one elephant). *Am. J. Anat.* 180, 126–142.
- S2. Tramo, M.J., Loftus, W.C., Thomas, C.E., Green, R.L., Mott, L.A., and Gazzaniga, M.S. (1995). Surface area of human cerebral cortex and its gross morphological subdivisions: *in vivo* measurements in monozygotic twins suggest differential hemisphere effects of genetic factors. *J. Cogn. Neurosci.* 7, 292–302.
- S3. Fischl, B., and Dale, A.M. (2000). Measuring the thickness of the human cerebral cortex from magnetic resonance images. *Proc. Natl. Acad. Sci. USA* 97, 11050–11055.
- S4. Stephan, H., Frahm, H., and Baron, G. (1981). New and revised data on volumes of brain structures in insectivores and primates. *Folia Primatol.* 35, 1–29.
- S5. Abeles. (1991). *Corticonics* (Cambridge: Cambridge University Press).
- S6. Braitenberg, V., and Schütz, A. (1998). *Cortex: Statistics and Geometry of Neuronal Connectivity*, Second Edition (Berlin: Springer).
- S7. Rockel, A.J., Hiorns, R.W., and Powell, T.P.S. (1980). The basic uniformity in structure of the neocortex. *Brain* 103, 221–244.
- S8. Haug, H. (1981). The use of stereology demonstrated by the evaluation of man's cerebral cortex. *Prog. Clin. Biol. Res.* 59B, 123–128.
- S9. Braendgaard, H., Evans, S.M., Howard, C.V., and Gundersen, H.J. (1990). The total number of neurons in the human neocortex unbiasedly estimated using optical disectors. *J. Microsc.* 157, 285–304.
- S10. Braak, H., and Braak, E. (1986). Ratio of pyramidal cells versus non-pyramidal cells in the human frontal isocortex and changes in ratio with ageing and Alzheimer's disease. In *Progressive Brain Research*, Volume 70, D.F. Swaab, E. Fliers, M. Mirmiran, W.A. Van Gool, and F. Van Haaren, eds. (Amsterdam: Elsevier), pp. 185–212.
- S11. Meinecke, D.L., and Peters, A. (1987). GABA immunoreactive neurons in rat visual cortex. *J. Comp. Neurol.* 261, 388–404.
- S12. McCormick, D.A., Connors, B.W., Lighthall, J.W., and Prince, D.A. (1985). Comparative electrophysiology of pyramidal and sparsely spiny stellate neurons of the neocortex. *J. Neurophysiol.* 54, 782–806.
- S13. Attwell, D., and Laughlin, S.B. (2001). An energy budget for signaling in the grey matter of the brain. *J. Cereb. Blood Flow Metab.* 21, 1133–1145.
- S14. Markram, H., Lübke, J., Frotscher, M., Roth, A., and Sakmann, B. (1997). Physiology and anatomy of synaptic connections between thick tufted pyramidal neurones in the developing rat neocortex. *J. Physiol.* 500, 409–440.
- S15. Hardingham, N.R., and Larkman, A.U. (1998). The reliability of excitatory synaptic transmission in slices of rat visual cortex *in vitro* is temperature dependent. *J. Physiol.* 507, 249–256.
- S16. Douglas, R.J., Koch, C., Mahowald, M., Martin, K.A.C., and Suarez, H.H. (1995). Recurrent excitation in neocortical circuits. *Science* 269, 981–985.
- S17. Allen, C., and Stevens, C.F. (1994). An evaluation of causes for unreliability of synaptic transmission. *Proc. Natl. Acad. Sci. USA* 91, 10380–10383.
- S18. Hille, B. (1992). *Ionic Channels of Excitable Membranes*, Second Edition (Sunderland, MA: Sinauer).
- S19. Stuart, G., and Spruston, N. (1998). Determinants of voltage attenuation in neocortical pyramidal neuron dendrites. *J. Neurosci.* 18, 3501–3510.
- S20. Braak, H. (1987). Architectonics as seen by lipofuscin stains. In *Cerebral Cortex*, Volume 1, A. Peters and E.G. Jones, eds. (New York: Plenum), pp. 59–104.
- S21. Mainen, Z.F., Joerges, J., Huguenard, J.R., and Sejnowski, T.J. (1995). A model of spike initiation in neocortical pyramidal neurons. *Neuron* 15, 1427–1439.
- S22. Elston, G.N., Benavides-Piccione, R., and DeFelipe, J. (2001). The pyramidal cell in cognition: a comparative study in human and monkey. *J. Neurosci.* 21, RC163.
- S23. Larkman, A.U. (1991). Dendritic morphology of pyramidal neurones of the visual cortex of the rat: III. Spine distributions. *J. Comp. Neurol.* 306, 332–343.
- S24. Sloper, J.J., and Powell, T.P. (1979). A study of the axon initial segment and proximal axon of neurons in the primate motor and somatic sensory cortices. *Philos. Trans. R. Soc. Lond. B. Biol. Sci.* 285, 173–197.
- S25. Feldman, M.L. (1984). Morphology of the neocortical pyramidal neuron. In *Cerebral Cortex*, Volume 1, A. Peters and E.G. Jones, eds. (New York: Plenum), pp. 123–200.
- S26. Schüz, A., and Demianenko, G.P. (1995). Constancy and variability in cortical structure. A study on synapses and dendritic spines in hedgehog and monkey. *J. Hirnforsch.* 36, 113–122.
- S27. Frey, K.A. (1994). Positron emission tomography. In *Basic Neurochemistry*, G.J. Siegel, B.W. Agranoff, R.W. Albers, and P.B. Molinoff, eds. (New York: Raven), pp. 935–955.